Processing and Application of Ceramics 12 [1] (2018) 1–7
https://doi.org/10.2298/PAC1801001V

Magnetic and electrical properties of Cr substituted Ni nano ferrites

Katrapally Vijaya Kumar[1,*], Rapolu Sridhar[2], Dachepalli Ravinder[3]

[1]*Department of Physics, JNTUH College of Engineering Sultanpur, Sultanpur (V), Pulkal (M), Sangareddy-Dist. 502293 Telangana State, India*
[2]*Department of BS&H, Vignan Institute of Technology & Science, Yadadri-Bhuvanagiri-Dist.508284, Telangana State, India*
[3]*Department of Physics, Osmania University, Hyderabad-500007, Telangana State, India*

Received 1 July 2017; Received in revised form 10 August 2017; Received in revised form 7 November 2017; Accepted 4 December 2017

Abstract

Nano-ferrites with composition $NiCr_xFe_{2-x}O_4$ (where x = 0.1, 0.3, 0.5, 0.7, 0.9, 1.0) were synthesized through citrate-gel auto combustion technique at moderately low temperature. X-ray analysis shows cubic spinel structure single phase without any impurity peak and average crystallite size in the range 8.5–10.5 nm. Magnetic properties were measured using a vibrating sample magnetometer at room temperature in the applied field of ±6 KOe. The obtained M-H loop area is very narrow, hence the synthesized nano ferrites are soft magnetic materials with small coercivity. Magnetic parameters such as saturation magnetization (M_s), coercivity (H_c), remanent magnetization (M_r) and residual magnetization were measured and discussed with regard to Cr^{3+} ion concentration. Electrical properties were measured using two probe method from room temperature to well beyond transition temperature. The DC resistivity variation with temperature shows the semiconductor nature. Resistivity, drift mobility and activation energy values are measured and discussed with regard to composition. The Curie temperature was determined using DC resistivity data and Loria-Sinha method. The observed results can be explained in detail on the basis of composition.

Keywords: *Ni-Cr ferrites, citrate-gel method, XRD, magnetic properties, electrical properties*

I. Introduction

Ferrites with general formulae of MFe_2O_4 are immense magnetic ceramics and better than pure metals due to their high electrical resistivity and lower cost [1,2]. Ferrites show the fascinating electrical and magnetic properties in the nanocrystalline form compared with those of bulk form. This is because of the cation distribution over tetrahedral and octahedral sites, which has a significant effect on the electrical and magnetic behaviour [3]. Hence, the cation distribution is distinctly different from ferrite nanoparticles compared to the bulk ferrites [4]. Accordingly, the ferrite nanoparticles are technically important promising materials due to various applications in electronics [5,6].

Nickel ferrite has an inverse spinel structure with Ni^{2+} in octahedral site and Fe^{3+} equally distributed among octahedral and tetrahedral sites [7]. These ferrites are very important materials designed for electronic devices, such as telecommunication tools, permanent magnets, magnetic media used in computers, recording devices and electronic and microwave devices because of their low eddy current losses and good magnetic properties [8].

The properties of ferrites are also dependent on preparation method, chemical composition and type of substituent [9]. Among several methods such as sol-gel route [10], co-precipitation [11], hydrothermal method [12] and reverse micelle technique [13] etc., the citrate-gel auto combustion method is one of the most attractive preparation methods for synthesis of nanosized ferrite particles. The reasons are low annealing temperature, short preparation time, good stoichiometry control and the production of ultrafine particles with a narrow size distribution. Divalent or trivalent substituted nickel nano ferrites are extensively used as magnetic materials in a wide range of technological applications [14].

The electrical and magnetic properties of the nano-

* Corresponding author: tel: +91 9000203797,
e-mail: *kvkphd@gmail.com*

sized ferrites play a vital role in different fields and they are dependent on several factors [15]. Substitution of Fe^{3+} with trivalent cations like Al^{3+} and Cr^{3+} is necessary to accomplish specific objectives like increase of resistivity and saturation magnetization decreases [16]. Several researchers have presented the influence of trivalent substitutions to improve their electrical and magnetic properties [17,18]. To the best of our knowledge, the electrical and magnetic properties of Cr^{3+} substituted nickel nano ferrite has not yet been investigated in detail. Therefore, in the present work, Cr substituted nickel nano ferrites of different compositions have been prepared by the citrate-gel auto combustion method. Further, the electrical properties of Cr substituted nickel nano ferrites have been investigated as a function of temperature, while the magnetic properties have been investigated as a function of composition at the room temperature.

II. Experimental procedure

2.1. Sample preparation

Cr-substituted Ni ferrites, having the general formula $NiCr_xFe_{2-x}O_4$ (where x = 0.1, 0.3, 0.5, 0.7, 0.9 and 1.0), were synthesized by using citrate-gel auto combustion method. In a typical experiment, analytically grade nickel nitrate ($Ni(NO_3)_2{\times}6\,H_2O$, 99% pure, AR Grade), chromium nitrate ($Cr(NO_3)_2{\times}3\,H_2O$, 99% pure, AR Grade), ferric nitrate ($Fe(NO_3)_2{\times}9\,H_2O$, 99% pure, AR Grade) and citric acid ($C_6H_8O_7{\times}H_2O$, 99% pure, GR Grade) were dissolved in sufficient amount of deionized water in stoichiometry proportions. To maintain the pH of the solution at 7, ammonia (NH_3), which acts as the precipitating agent was added to the solution kept under constant stirring. The resulting solution was then heated at 80 °C until it transformed into wet gel. Then the gel was ignited in a self-propagating combustion manner to form a fluffy loose powder. The as-burnt ferrite powders were pulverised in agate mortar and calcined in muffle furnace at 700 °C for 5 h. The calcined ferrite powders were again ground in agate mortar to obtain a fine ferrite powder.

2.2. Materials characterization

The structural characterization was done by a Bruker D8 Advance X-ray diffractometer with Cu Kα radiation source (λ = 0.15405 nm) between the Bragg angles 20° to 80° in steps of 0.04°/s. The average crystallite size was calculated using the Scherrer formula for the high intensity 311 peak [19]. The morphology and average crystallite size were characterized by TEM (Tecnai-12, FEI, Netherlands).

Magnetic properties were determined from the obtained hysteresis loops by using vibrating sample magnetometer (VSM) GMW 3473 in the range ±6 kOe applied field at room temperature. From the obtained hysteresis loops, the saturation magnetizations (M_s), remenant magnetization (M_r), coercivity (H_c) were determined and magnetic moment (μ_B) was calculated using the relation [20]:

$$\mu_B = \frac{M_w \cdot x \cdot M_s}{5585} \tag{1}$$

where M_w is the molecular weight of each composition. The anisotropy constant (K) was calculated by using the relation [21]:

$$H_c = \frac{0.98K}{M_s} \tag{2}$$

For electrical measurements, the prepared samples were pressed into a circular disc shaped pellets (~10 mm diameter and ~2 mm thickness) and these pellets were sintered at 400 °C for 4 hours. The prepared pellets are silver coated on both sides and air dried to have good ohmic contact. The DC resistivity was measured as a function of temperature by using the two-probe method [22]. The relationship between resistivity and temperature may be expressed as [23]:

$$\rho = \rho_0 \cdot \exp \frac{\Delta E}{k_B T} \tag{3}$$

where ρ is the DC electrical resistivity at temperature T, k_B is the Boltzmann constant and ΔE is the activation energy. The drift mobility of the charge carriers is calculated from the electrical resistivity data by the following equation [24]:

$$\mu = \frac{1}{n \cdot e \cdot \rho} \tag{4}$$

where n is the number of charge carriers, e is the charge of electron, ρ is the resistivity at a given temperature.

III. Results and discussion

3.1. Structural properties

X-ray diffraction patterns of the mixed $NiCr_xFe_{2-x}O_4$ nano ferrite system are shown in Fig. 1. The appearance of the (111), (220), (311), (400), (511), (440) and (533) planes corresponding to the cubic spinel structure, matches with the standard reference data PDF# 862267 for nickel ferrites ($NiFe_2O_4$) from the international centre for diffraction data (ICDD) and all the samples have shown cubic spinel structure being single phase [25]. The average crystallite size is in the range of 8.5 nm to 10.5 nm. Micrographs of $NiCr_{0.3}Fe_{1.7}O_4$ and $NiCr_{0.7}Fe_{1.3}O_4$ nano ferrite are represented in Figs. 2 and 3. Micrographs point out the nanostructure environment with the crystallite size in nanometre range.

3.2. Magnetic properties

M-H hysteresis loops

The hysteresis loops are obtained for all samples in the range ±6 kOe applied field at room temperature using VSM. The obtained hysteresis loops are illustrated

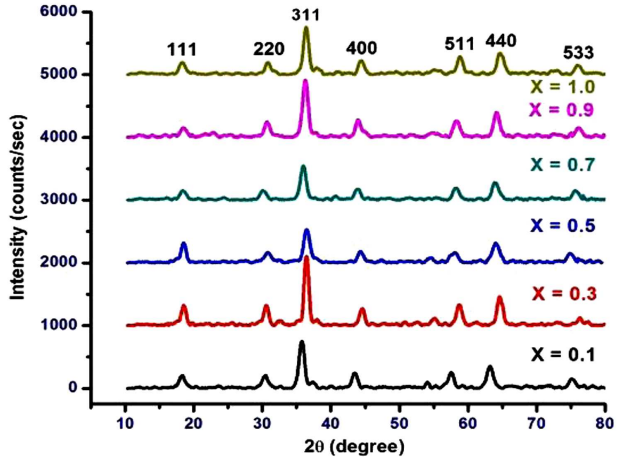

Figure 1. XRD pattern of $NiCr_xFe_{2-x}O_4$ nano ferrite system

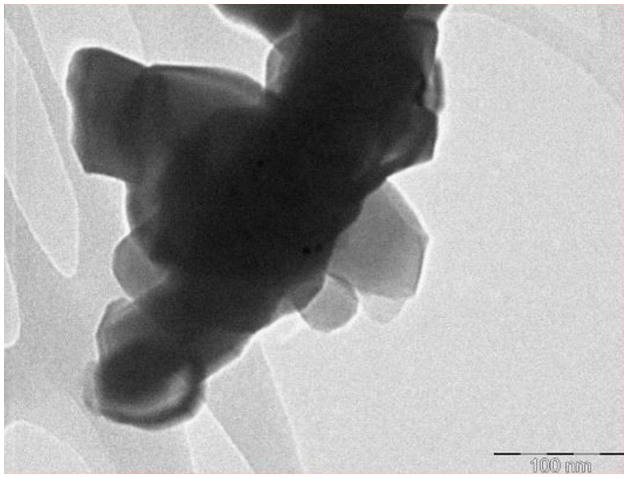

Figure 2. TEM image of $NiCr_{0.3}Fe_{1.7}$ nano ferrite

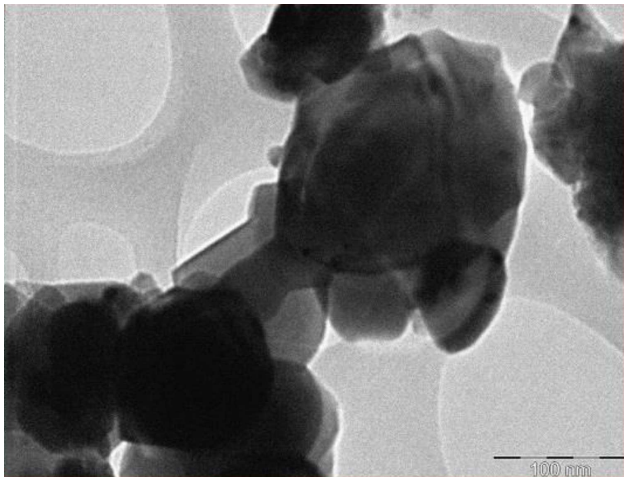

Figure 3. TEM image of $NiCr_{0.7}Fe_{1.3}O_4$ nano ferrite

in Fig. 4. The loop area is very narrow therefore the samples present soft ferrite nature with small coercivity [26]. Hence it is clear that Cr substitution in Ni ferrites has enhanced soft magnetic performance. So these materials may be desirable for transformers to minimize the energy dissipation with the alternating fields associated with AC electrical applications. Several magnetic parameters, such as saturation magnetization (M_s), coercivity (H_c), remanent magnetization (M_r) and residual magnetization ratio (M_r/M_s), are directly extracted from hysteresis curves. The magnetic moment (μ_B) and anisotropy constant (K) were determined from the saturation magnetization and coercivity data and reported in Table 1.

Saturation magnetization and magnetic moment

Microstructure of the materials and composition greatly influence the magnetic properties of soft ferrites. In the prepared sample, magnetization comes from the interchange of domain walls movement, spin rotation and a sum of exchange interactions between A-site and B-site of the ferrite [27]. From the hysteresis loops, it is observed that the Ni-Cr nano ferrites have lower saturation magnetization and coercivity due to the small grain size [28].

The saturation magnetization (Ms) decreases from 4.49 to 2.97 emu/g with increase of Cr^{3+} concentration in Ni nano ferrites (Table 1 and Fig. 5). It may be explained with low magnetic moment Cr^{3+} ions (~3 μ_B) being substituted in place of higher magnetic moment

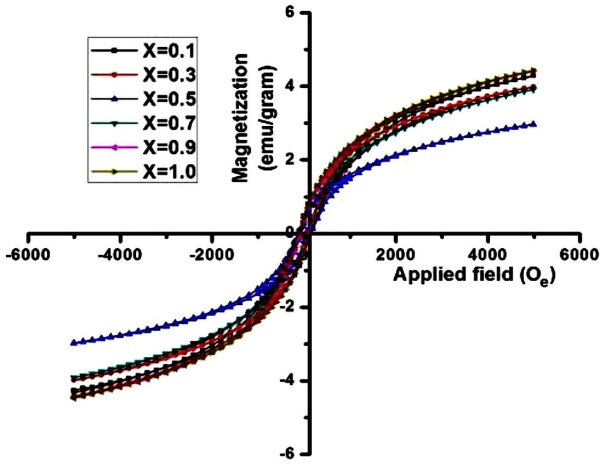

Figure 4. M-H loops of $NiCr_xFe_{2-x}O_4$ nano ferrite system

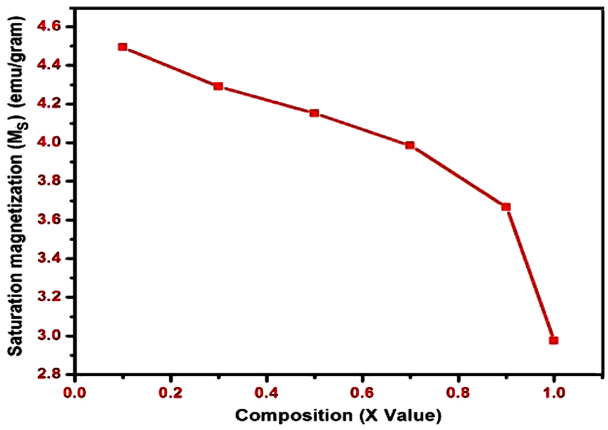

Figure 5. Saturation magnetization variation with composition (x)

Table 1. Magnetic properties (saturation magnetization M_s, remanent magnetization M_r, residual magnetization ratio M_r/M_s, magnetic moment μ_B, coercitive field H_c and anisotropy constant K) of $NiCr_xFe_{2-x}O_4$ nano ferrite system

x	Crystallite size [nm]	M_s [emu/g]	M_r [emu/g]	M_r/M_s	μ_B	H_c [Oe]	K [emu/Oe]
0.1	8.96	4.49	0.51	0.113	0.188	136.2	624.5
0.3	10.36	4.29	0.47	0.110	0.179	126.0	551.4
0.5	7.95	4.15	0.39	0.094	0.172	116.6	493.9
0.7	8.55	3.99	0.24	0.060	0.165	63.0	256.3
0.9	8.84	3.67	0.35	0.095	0.151	79.2	296.2
1	9.26	2.97	0.44	0.150	0.122	106.1	321.9

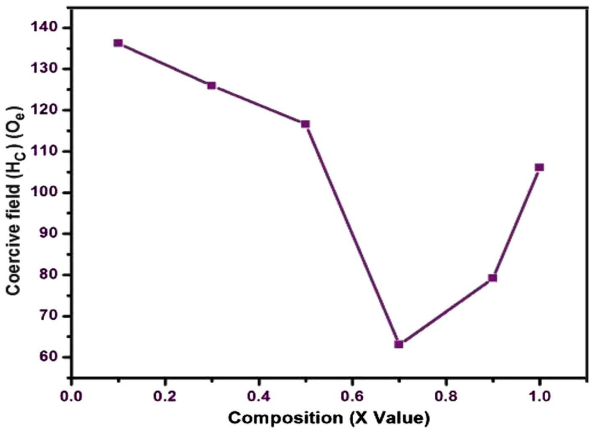

Figure 6. Coercive field variation with composition (x)

Fe^{3+} ions (~5 μ_B) in the octahedral (B-site) sub lattice of the ferrite. The increase of Cr^{3+} ion concentration decreases Fe^{3+}(B)/Fe^{2+}(A) ratio. This causes the decrease in the A-B super exchange interaction [29], which leads to the decrease of saturation magnetization. This decrease in the saturation magnetization is ascribed to the weak magnetic interactions in Ni-Cr ferrites.

The calculated magnetic moment values are tabulated in Table 1. It is clear that the magnetic moment values decrease from 0.188 μ_B to 0.122 μ_B with the increase of Cr^{3+} ion concentration in Ni nano ferrites. This can be attributed to a greater tendency of Cr^{3+} ions for B sites. Therefore, all these results show that materials are getting changed into soft ferrite materials.

Coercivity and anisotropy constant

From the hysteresis loops the coercivity values are measured and reported in Table 1. It is clear that the coercivity value decreases from 136.2 Oe to 63.0 Oe followed by its increase to 106.1 Oe with the increase Cr^{3+} concentration in Ni nano ferrites (Fig. 6). The decrease in coercivity with the increase in Cr^{3+} ion concentrations due to the decrease in anisotropy field happening in order to minimize the domain wall energy [30]. In case of x = 0.9 and 1.0 ferrite compositions coercivity value increases due to the increase in the magnetic crystalline anisotropy.

The calculated anisotropy constants (K) are presented in Table 1. It is seen that the value of anisotropy constant (K) decreases from 624.5 emu/Oe to 256.3 emu/Oe and after that increases to 321.9 emu/Oe with the increase of the Cr^{3+} concentration in Ni nano ferrites.

The remanent magnetization (M_r) and residual magnetization ratio (M_r/M_s) values are given in Table 1. Remanent magnetization (M_r) varies between 0.24 emu/g and 0.51 emu/g with the residual magnetization ratio (M_r/M_s) values between 0.060 and 0.150 with Cr^{3+} ion concentration. The low value of residual magnetization ratio implies on the isotropic nature of the prepared ferrite samples. The low values of the remanent magnetization (M_r) can be accredited to the low saturation magnetization as well as the nanosized characteristics [31]. Materials with such low residual magnetisation could be used for low inductance cores and coils [32].

3.3. Electrical properties

DC resistivity variation with temperature

The DC resistivity variation with temperature for $NiCr_xFe_{2-x}O_4$ nano ferrite system is shown in Fig. 7. It is observed that the resistivity linearly decreases with increase in temperature due to the hopping of electrons, which indicates the semiconductor nature [33]. In the present system the conduction process can be explained by the Verway and Boer mechanism [34]. During the sintering process a small amount of Fe^{2+} and Ni^{3+} ions are formed and electron exchange occurs between Fe and Ni ions, which can be represented as:

$$Ni^{2+} + Fe^{3+} \longleftrightarrow Ni^{3+} + Fe^{2+} \quad (5)$$

The conduction at low temperature (i.e. <400 K) is

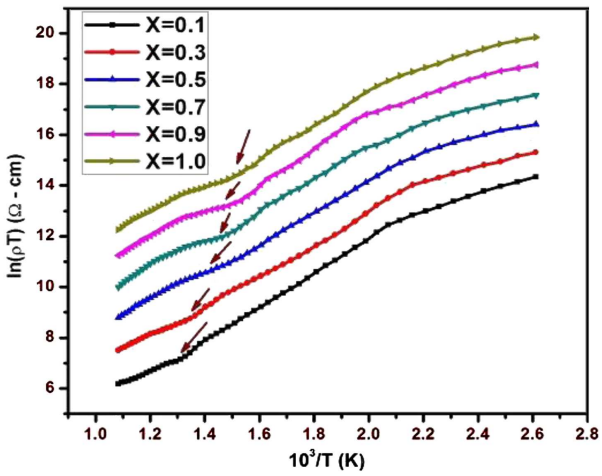

Figure 7. DC resistivity variation with inverse temperature (the Curie temperatures are indicated with arrows)

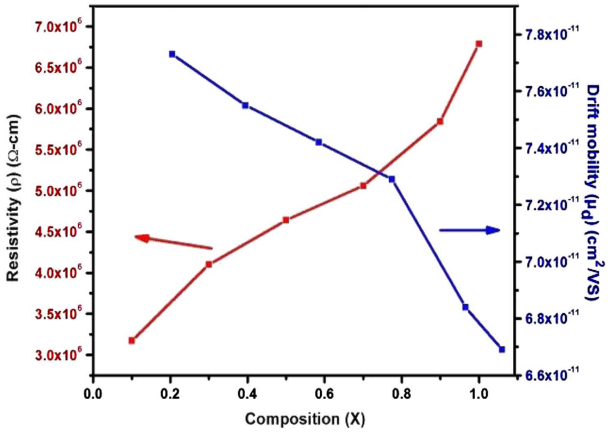

Figure 8. Resistivity and drift mobility variation with composition (x)

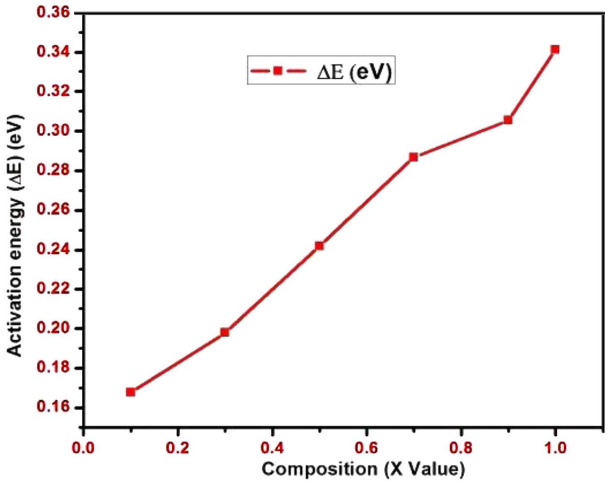

Figure 9. Activation energy variation with composition (x)

due to impurities, whereas at higher temperatures (i.e. >400 K) it is due to polaron hopping. Similar behaviour is also observed by other researchers [35,36].

DC resistivity and drift mobility

The variation of electrical resistivity and drift mobility with Cr^{3+} concentration are shown in Fig. 8. Electrical resistivity increases from 3.17×10^6 Ω·cm to 6.79×10^6 Ω·cm and the drift mobility decreases from 7.73×10^{-11} cm^2/V·s to 6.69×10^{-11} cm^2/V·s with the increases of Cr^{3+} ion concentration in Ni nano ferrite as evidenced in Table 2. It may be due to the hopping of electrons between $Fe^{3+}\leftrightarrow Fe^{2+}$ ions [34]. In the spinel structure the Ni^{2+} ions occupy octahedral (B) sites, Fe^{3+} ions are occupying both the octahedral (B) and tetrahedral (A) sites and the Cr^{3+} ions occupy the octahedral (B) sites [37]. The conduction mechanism in ferrites depends on the hopping of electrons between $Fe^{3+}\leftrightarrow Fe^{2+}$ at the octahedral (B) sites. Compared with B-B sites, the hopping of electrons is less probable between A-B sites and does not exist between A-A sites. Therefore only Fe^{3+} ions are present at A-sites while Fe^{2+} ions are created during the process and occupy B-sites [38]. However, Cr^{3+} ions occupy octahedral (B) site and as a result they decrease the Fe^{3+} ions at the B-sites. In turn, $Fe^{3+}\leftrightarrow Fe^{2+}$ ions polaron hopping happens [39,40]. Hence, increase in resistivity with increasing Cr^{3+} ion concentration. Similar trend observed in Co-Cr nano ferrite was previously reported [41]. The decrease in the drift mobility with composition is due to the fact that samples with higher resistivity have lower mobility and vice versa. Similar results observed in Co-Cr ferrites by Naeem Ashiq [42]. This shows that the investigated materials could be a good choice for high frequency applications.

Activation energy variation with composition

Activation energy could be calculated from the slope of $\ln(\rho \cdot T)$ with inverse temperature shown in Fig. 7. The computed activation energy values are presented in Table 2. Activation energy values are higher in the paramagnetic region as compared to the ferrimagnetic region. It can be attributed to the spin disordered states of the paramagnetic region and the spin ordered states of the ferrimagnetic region [43]. These results suggest that the change in the magnetic ordering has an effect on the conduction process [44]. On the other hand, the activation energy values indicate the slow polaron hopping conduction mechanism in ferrites.

The activation energy (ΔE) of each sample is presented in Table 2 and plotted in Fig. 9. It shows that activation energy (ΔE) increases with the increase of Cr^{3+} ion concentration. It may be due to the increase in resistivity with the increase in Cr^{3+} ion concentration, because activation energy acts in similar way to DC

Table 2. Electrical properties of $NiCr_xFe_{2-x}O_4$ nano ferrite system (activation energy in para region E_P, activation energy in ferro region E_F and activation energy ΔE)

x	Resistivity [Ωcm]	Drift mobility, μ_d [cm^2/V·s]	Activation energy [eV]			Curie temperature [K]	
			E_P	E_F	ΔE	From DC resistivity	Loria-Sinha technique
0.1	3.17×10^6	7.73×10^{-11}	0.41	0.24	0.16	775.4	789
0.3	4.10×10^6	7.55×10^{-11}	0.52	0.32	0.19	747.6	762
0.5	4.64×10^6	7.42×10^{-11}	0.63	0.39	0.24	705.3	729
0.7	5.06×10^6	7.29×10^{-11}	0.72	0.44	0.28	690.7	697
0.9	5.84×10^6	6.84×10^{-11}	0.79	0.48	0.30	659.5	678
1.0	6.79×10^6	6.69×10^{-11}	0.85	0.51	0.34	635.3	642

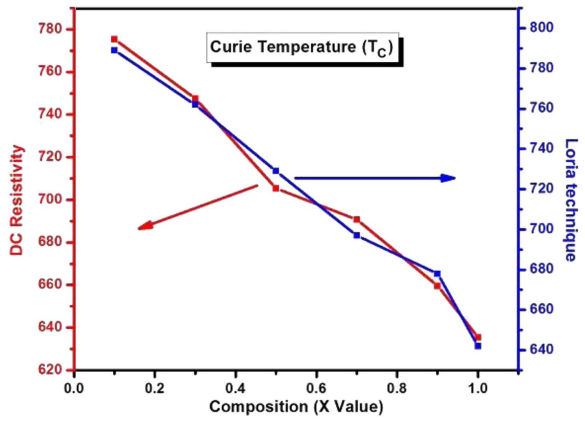

Figure 10. Curie temperature variation with composition (x)

electrical resistivity, as reported by others [45,46]. This increase in activation energy imply that the Cr ions entering into octahedral sites hinder the electron hopping between $Fe^{3+} \leftrightarrow Fe^{2+}$ ions lowering electrical conduction by obstruction of Fe^{2+} and Fe^{3+} transformation. Accordingly, the sample with higher resistivity has higher values of activation energies and vice versa [47].

Curie temperature

Arrhenius plot of $\ln(\rho \cdot T)$ *vs.* $10^3/T$ (Fig. 7) show change in slope. This indicates transformation from ferrimagnetic into paramagnetic phase at the temperature known as the Curie temperature. The obtained values of the Curie temperature are shown in Table 2 and Fig. 10. A decrease is observed on increasing the Cr^{3+} concentration, because the Fe^{3+} ions are replaced by paramagnetic Cr^{3+} ions [39]. The Curie temperature is determined by an overall strength of the exchange interaction between A and B sublattice. When the replacement of Fe^{3+} ion with Cr^{3+} ions increases, the magnetization decreases in B-sublattice without disturbing the A-sublattice. This leads to a decrease in the A-B interactions (Fe^{3+}–O^{2-}–Fe^{3+}) which results in the decrease of the Curie temperature. Similar behaviour was already observed for the trivalent substitution in nano ferrite system [48,49]. The Curie temperatures obtained from DC resistivity measurements were in good agreement with those recognised as the magnetic transition temperature (789 to 642 K) from the Loria-Sinha method (gravity method) as reported in Table 2.

IV. Conclusions

$NiCr_xFe_{2-x}O_4$ (where x = 0.1, 0.3, 0.5, 0.7, 0.9, 1.0) was synthesized using citrate-gel auto combustion method. X-ray diffraction pattern confirms the formation of the cubic spinel structure single phase without any impurity peaks with the crystallite size in the range of 8.5 to 10.5 nm. The obtained hysteresis loops confirm that the prepared Ni-Cr nano ferrites are soft magnets with narrow loop area and small coercivity. Hence, these materials may be desirable for transformers to minimize the energy dissipation. The DC resistivity variation with temperature shows the semiconductor nature of the material. The increase in the resistivity and decrease in the drift mobility with Cr^{3+} ion concentration were ascribed to the electron hopping between $Fe^{3+} \leftrightarrow Fe^{2+}$ ions. This shows that materials may be good choice for high frequency applications. The sample with higher resistivity has higher values of activation energy for conductivity and vice versa. The measured Curie temperatures from DC resistivity were in good agreement with those obtained as magnetic transition temperatures from Loria-Sinha method.

Acknowledgement: The authors are grateful to Head, Department of Physics, Osmania University, Hyderabad for providing the facility to synthesis of samples. One of the authors (KVK) is grateful to Dr. B. Balu Naik, Principal JNTUH College of Engineering, Sultanpur, Pulkal (M), Sangareddy District and the author (RS) is grateful to Dr. G. Durga Sukumar Principal, Vignan Institute of Technology & Science, Yadadri-Bhuvanagiri (Nalgonda).

References

1. S.S. Ata-Allah, M. Kaiser, "Conductivity and dielectric studies of copper-aluminate substituted spinel nickel ferrite", *J. Alloys Compd.*, **471** (2009) 300–309.
2. N.M. Deraza, M.M. Hessien, "Structural and magnetic properties of pure and doped nanocrystalline cadmium ferrite", *J. Alloys Compd.*, **475** (2009) 832–839.
3. M.F.A. Hilli, S. Li, K.S. Kassim, "Microstructure, electrical properties and Hall coefficient of europium-doped Li-Ni ferrites", *Mater. Sci. Eng. B*, **158** (2009) 1–6.
4. N. Sivakumar, A. Narayanasamy, K. Shinoda, C.N. Chinnasamy, B. Jayadevan, "Electrical and magnetic properties of chemically derived nanocrystalline cobalt ferrite", *J. Appl. Phys.*, **102** (2007) 013916.
5. A. Vermaa, M.L. Alama, R. Chatterjeea, T.C. Goelb, R.G. Mendirattac, "Development of a new soft ferrite core for power applications", *J. Magn. Magn. Mater.*, **300** (2006) 500–505.
6. A. Goldman, *Handbook of Modern Ferromagnetic Materials*, Kluwer Academic Publishers, Boston, USA, 1999.
7. Kh. Roumaiah, "The transport properties of the mixed Ni-Cu ferrite", *J. Alloys Compd.*, **465** (2008) 291–195.
8. M.H. Khedr, "Isothermal reduction kinetics at 900–1100 °C of $NiFe_2O_4$ sintered at 1000–1200 °C", *J. Anal. Appl. Pyrol.*, **73** (2005) 123–129.
9. A. Ataie, I.R. Harris, C.B. Ponton, "Magnetic properties of hydrothermally synthesized strontium hexaferrite as a function of synthesis conditions", *J. Mater. Sci.*, **30** (1995) 1429–1433.
10. A. Chatterjee, D. Das, S.K. Pradhan, D. Chakravarty, "Synthesis of nanocrystalline nickel-zinc ferrite by the sol-gel method", *J. Magn. Magn. Mater.*, **127** (1993) 214–218.
11. M. Pal, D. Chakravorty, "Nanocrystalline magnetic alloys and ceramics", *Sadhana*, **28** (2003) 283–297.
12. A. Dias, "Microstructural evolution of fast-fired nickel-zinc ferrites from hydrothermal nanopowders", *Mater. Res. Bull.*, **35** [9] (2000) 1439–1446.
13. S. Gubbala, H. Nathani, K. Koizol, R.D.K. Misra, "Magnetic properties of nanocrystalline Ni-Zn, Zn-Mn, and Ni-Mn ferrites synthesized by reverse micelle technique",

Physica B, **348** [1-4] (2004) 317–328.
14. B. Visuanathan, V.R.K. Murthy, *Ferrites Materials Science and Technology*, Narosa Publishing House, New Delhi, India, 1990.
15. K. Kondo, T. Chiba, S. Yamada, "Effect of microstructure on magnetic properties of Ni-Zn ferrites", *J. Magn. Magn. Mater.*, **254-255** (2003) 541–543.
16. R.C. Kambale. N.R. Adhate, B.K. Chougule, Y.d. Kolekar, "Magnetic and dielectric properties of mixed spinel Ni-Zn ferrites synthesized by citrate nitrate combustion method", *J. Alloys Compd.*, **507** (2010) 372–377.
17. P.P. Hankare, V.T. Vader, N.M. Patiletal, "Synthesis, characterization and studies on magnetic and electrical properties of Mg ferrite with Cr substitution", *Mater. Chem. Phys.*, **113** [1] (2009) 233–238.
18. S. Bhukal, T. Namgyal, S. Mor, S. Bansal, S. Singhal, "Structural, electrical, optical and magnetic properties of chromium substituted Co-Zn nanoferrites $Co_{0.6}Zn_{0.4}Cr_xFe_{2-x}O_4$ ($0 \leq x \leq 1.0$) prepared via sol-gel auto-combustion method", *J. Mol. Struct.*, **1012** (2012) 162–167.
19. B.D. Cullity, *Elements of X-Ray Diffraction*, Addison Weseley Publishing, Reading, 1959, pp. 132-133.
20. R.C. Kambale, P.A. Shaikh, S.S. Kamble, Y.D. Kolekar, "Effect of cobalt substitution on structural, magnetic and electric properties of nickel ferrite", *J. Alloy Compd.*, **478** (2009) 599–603.
21. D.R. Mane, D.D. Birajdar, Sagar E. Shirsath, R.A. Telugu, R.H. Kadam, "Structural and magnetic characterizations of Mn-Ni-Zn ferrite nanoparticles", *Phys. Status Solidi A*, **207** (2010) 2355–2363.
22. C.B. Kolekar, P.N. Kamble, S.G. Kulkarni, "Effect of Gd^{3+} substitution on dielectric behaviour of copper-cadmium ferrites", *J. Mater. Sci.*, **30** [22] (1995) 5784–5788.
23. S.O. Kasap, *Principles of Electronic Materials and Devices*, New York, McGraw-Hill, 2006.
24. M.N. Ashiq, N. Bibi, M.A. Malana, "Effect of Sn-Ni substitution on the structural, electrical and magnetic properties of mixed spinel ferrites", *J. Alloy Compd.*, **490** (2010) 594–597.
25. R.S. Devan, Y.D. Kolekar, B.K. Chougule, "Effect of cobalt substitution on the properties of nickel-copper ferrite", *J. Phys., Condens. Matter.*, **18** (2006), 9809–9821.
26. S.A. Mazen, A.M. Abdel-Daiem, "IR spectra and dielectric properties of Cu-Ge ferrite", *Mater. Chem. Phys.*, **130** (2011) 847–852.
27. O. Caltun, I. Dumitru, M. Feder, N. Lupu, "Substituted cobalt ferrites for sensors applications", *J. Magn. Magn. Mater.*, **320** (2008) 869–873.
28. X. Qi, J. Zhou, Z. Yue, Z. Gui, L. Li, "Effect of Mn substitution on the magnetic properties of MgCuZn ferrites", *J. Magn. Magn. Mater.*, **251** (2002) 316–322.
29. I.H. Gul, A. Maqsood, "Structural, magnetic and electrical properties of cobalt ferrites prepared by the sol-gel route", *J. Alloy. Compd.*, **465** (2008) 227–231.
30. Y.M. Yokovlev, L.B. Rubarikaya, N. Lapovok, "Ferromagnetic resonance in lithium ferrite", *Sov. Phys. Solid State*, **10** (1969) 2301–2303.
31. A.I. Borhan, T. Slatineanu, A.R. Iordan, M.N. Palamaru, "Influence of chromium ion substitution on the structure and properties of zinc ferrite synthesized by the sol-gel auto-combustion method", *Polyhedron*, **56** (2013) 82–89.
32. L. Gama, E.P. Hernandez, D.R. Cornejo, A.A. Costa, S.M. Rezende, R.H.G.A. Kimimami, A.C.F.M. Costa, "Magnetic and structural properties of nanosize Ni-Zn-Cr ferrite particles synthesized by combustion reaction", *J. Magn. Magn. Mater.*, **317** (2007) 29–33.
33. J.W. Verwey, J.H. De Boer, "Cation arrangement in a few oxides with crystal structures of the spinel type", *Rec. Trav. Chim. Pays-B*, **55** (1936) 531–540.
34. M.J. Iqbal, M.R. Siddiquah, "Structural, electrical and magnetic properties of Zr-Mg cobalt ferrite", *J. Magn. Magn. Mater.*, **320** (2008) 845–850.
35. M.Z. Said, D.M. Hemeda, S. Abdel Kadar, G.Z. Farag, "Structural, electrical and infrared studies of $Ni_{0.7}Cd_{0.3}Sm_xFe_{2-x}O_4$ ferrite", *Turk. J. Phys.*, **31** (2007) 41–50.
36. T.J. Shinde, A.B. Gadkari, P.N. Vasambekar, "Influence of Nd^{3+} substitution on structural, electrical and magnetic properties of nanocrystalline nickel ferrites", *J. Alloy Compd.*, **513** (2012) 80–85.
37. M.J. Iqbal, M.R. Siddiquah, "Electrical and magnetic properties of chromium substituted cobalt ferrite nano materials", *J. Alloy. Compd.*, **453** (2008) 513–518.
38. A.L. Lakshman, P.S.V. Subba Rao, P. Wara, "Electrical properties of In^{3+} and Cr^{3+} substituted magnesium-manganese ferrites", *J. Phys. D. Appl. Phys.*, **38** (2005) 673–678.
39. A. Lakshman, K.H. Rao, R.G. Mendiratta, "Magnetic properties of In^{3+} and Cr^{3+} substituted Mg-Mn ferrites", *J. Magn. Magn. Mater.*, **250** (2002) 92–97.
40. L.C.F. Blackman, "Low loss magnesium manganese ferrites", *J. Electron. Control*, **2** [5] (1957) 451–456.
41. M.J. Iqbal, Z. Ahmad, T. Meydan, Y. Melikhov, "Physical, electrical and magnetic properties of nano-sized Co-Cr substituted magnesium ferrites", *J. Appl. Phys.*, **111** (2012) 033906.
42. M.N. Ashiq, F. Naz, M.A. Malana, R.S. Gohar, Z. Ahmad, "Role of Co-Cr substitution on the structural, electrical and magnetic properties of nickel nano-ferrites synthesized by the chemical co-precipitation method", *Mater. Res. Bull.*, **47** (2012) 683–686
43. M. El-Shabasy, "DC electrical properties of Zn-Ni ferrites", *J. Magn. Magn. Mater.*, **172** (1997) 188–192.
44. B.K. Bammannavar, L.R. Naik, R.B. Pujar, B.K. Chougale, "Influence of time and temperature on resistivity and microstructure of $Cu_xCo_{1-x}Fe_2O_4$ mixed ferrites", *Prog. Electromagn. Res. Lett.*, **14** (2008) 121–123.
45. N. Rezlescu, E. Rezlescu, P.D. Popa, L. Rezlescu, "Effects of rare-earth oxides on physical properties of Li-Zn ferrite", *J. Alloys Compd.*, **275-277** (1998) 657–659.
46. I.H. Gul, E. Pervaiz, "Comparative study of $NiFe_{2-x}Al_xO_4$ ferrite nanoparticles synthesized by chemical co-precipitation and sol-gel combustion techniques", *Mater. Res. Bull.*, **47** (2012) 1353–1361.
47. B. Ramesh, D. Ravinder, "Electrical properties of Li-Mn ferrites", *Mater. Lett.*, **62** (2008) 2043–2046.
48. S.S. Ata-Allah, "Influence of Ga substitution on the magnetic and electric behaviour of $Cu_{0.5}Zn_{0.5}Fe_2O_4$ compound", *J. Magn. Magn. Mater.*, **284** (2004) 227–238.
49. M.A. Gabal, Y.M. AlAngari, "Low-temperature synthesis of nanocrystalline NiCuZn ferrite and the effect of Cr substitution on its electrical properties", *J. Magn. Magn. Mater.*, **322** (2010) 3159–3165.